

# Parallel Temperatures in Supersonic Beams: Ultra Cooling of Light Atoms Seeded in a Heavier Carrier Gas.

A. Miffre, M. Jacquey, M. Büchner, G. Trénec and J. Vigué

*Laboratoire Collisions Agrégats Réactivité -IRSAMC*  
*Université Paul Sabatier and CNRS UMR 5589*  
*118, Route de Narbonne 31062 Toulouse Cedex, France*  
*e-mail: jacques.vigue@irsamc.ups-tlse.fr*  
 (Dated: September 19, 2018)

## Abstract

Supersonic expansion is a very powerful tool to produce an atomic beam with a well defined velocity and, by seeding a test gas in such an expansion, the energy of the test gas can be transferred, at least partially, to the very-low-temperature carrier gas. The case usually studied is the one of a heavy gas seeded in a light carrier gas and, in this case, the parallel temperature of the seeded gas is always larger than the one of the carrier gas. In the present paper, we study the opposite case which has received less attention: when a light gas is seeded in a heavier carrier gas, the parallel temperature can be substantially lower for the seeded gas than for the carrier gas. This effect has been first observed by Campargue and coworkers in 2000, in the case of atomic oxygen seeded in argon. In the present paper, we develop a theoretical analysis of this effect, in the high dilution limit, and we compare our theoretical results to several experimental observations, including a set of measurements we have made on a beam of lithium seeded in argon. The agreement between theory and experiments is good.

## I. INTRODUCTION

We have recently observed that, in a supersonic beam of argon seeded with lithium, the parallel temperature of lithium is roughly one third of the parallel temperature of argon [1]. A similar effect was reported in 2000 by Campargue and co-workers [2] on a beam of atomic oxygen seeded in argon: the oxygen parallel temperature was close to half the argon parallel temperature. This result was found to be in agreement with a calculation developed by the same authors.

This effect is surprising because one would naively expect that the parallel temperature of the seeded gas cannot be lower than the parallel temperature of the carrier gas: the expansion of the carrier gas is the source of the cooling effect and the energy of the seeded gas is transferred by collisions to the carrier gas, but the transfer should not be complete. This view is too naive as shown below, but it is supported by all the experiments involving a heavy gas seeded in a light carrier gas: the parallel temperature of the seeded gas always exceeds the one of the carrier gas and the ratio of these two temperatures increases steadily with the mass ratio, from 2.2 – 2.5 for an He-Ar mixture, up to 4 – 4.5 for He-Xe mixture, and reaching 13 – 15 for H<sub>2</sub>-Xe mixture, following results due to Campargue and co-workers [3, 4]. At the same time, the mean velocities of the two components are different and this difference, the velocity slip effect [5, 6], increases also with the mass ratio.

The theory giving the terminal temperatures in supersonic beams of a pure monoatomic gas was developed by many authors including Anderson and Fenn [7], Hamel and Willis [8], Knuth and Fisher [9], Miller and Andres [6], Toennies and Winkelmann [10] and by Beijerinck and Verster [11]. The extension to the case of binary mixtures was made by Cooper and Bienkowski [12], by Anderson and coworkers [5, 14], by Chesneau and Campargue [17] (the subject has been reviewed by D.R. Miller [13]). Because a large majority of experiments corresponds to a heavy species seeded in a light carrier gas, the calculations were done in this case (reference [2] being an exception). These calculations established that the terminal parallel temperatures of the two species are not equal [14] and were able to explain the observed ratio of parallel temperatures of the seeded and carrier gas [15, 16, 17]. In the present paper, we apply this theory to the case of mixtures of monoatomic gases. We need several approximations to make an analytic theory and the most important one consists in neglecting the velocity slip effect. This approximation is good when the seeded gas atomic mass  $m_2$  is smaller than or comparable to the one of the carrier gas  $m_1$ . We are able to calculate the ratio of parallel temperatures of the seeded and carrier gases, as a function of their interaction potentials and atomic masses.

This theory provides a physical explanation of the ultra cooling effect: during a supersonic expansion of a pure gas, the basic phenomenon is the geometrical cooling effect of the perpendicular temperature, as illustrated by figure 1 of reference [10], and this cooling effect is transferred by collisions to the parallel temperature. When a gas is seeded in such an expansion, with a high dilution, the parallel temperature of the seeded gas is coupled to its own perpendicular temperature as well as to the parallel and perpendicular temperatures of the carrier gas. At the end of the expansion, the perpendicular temperatures of the seeded and carrier gases keep on decreasing and become considerably lower than the parallel temperature of the carrier gas which is frozen. Therefore, the terminal parallel temperature of the seeded gas can become lower than the same quantity for the carrier gas, provided that the collisional coupling of the temperatures acts for a longer time for the seeded gas than for the carrier gas. We must compare the efficiency of collisional exchange of kinetic energy

during the various possible collisions. Two effects govern this comparison: i) the relative ranges of the seeded gas-carrier gas interaction and the interaction between two atoms of the carrier gas; ii) the mass ratio as it plays a very important role in the way energy is redistributed during a collision. Among these two effects, the mass ratio usually dominates and we predict that the parallel temperature of the seeded gas can be considerably lower than the parallel temperature of the carrier gas when  $m_2 \ll m_1$ .

The present paper is organized as follows. We first recall the theory of the terminal temperatures in a pure gas expansion, thus introducing the needed ideas, notations and equations. Then, we generalize this calculation to the case of a gas mixture, in the limit of a high dilution. In the final part, we compare the available experiments with our calculations.

## II. TERMINAL PARALLEL TEMPERATURE IN SUPERSONIC EXPANSION OF A PURE MONOATOMIC GAS

In this part, we briefly recall the theory following the 1977 paper of Toennies and Winkelmann [10] (noted below TW) and we introduce the simplifications used by Beijerinck and Verster [11] in 1981 (noted below BV).

### A. Equations describing the cooling effect during a supersonic expansion

The starting point is the Boltzmann equation in the steady state regime:

$$\mathbf{v} \cdot \mathbf{grad} [n(\mathbf{r})f(\mathbf{r}, \mathbf{v})] = \left( \frac{\partial (nf)}{\partial t} \right)_{coll} \quad (1)$$

$n(\mathbf{r})$  is the gas density and  $f(\mathbf{r}, \mathbf{v})$  the normalized velocity distribution. Following TW, the supersonic expansion is approximately described, near its axis, by a spherically symmetric flow. The velocity distribution is assumed to remain Maxwellian, with different parallel and perpendicular temperatures  $T_{\parallel}$  and  $T_{\perp}$ :

$$f(\mathbf{r}, \mathbf{v}) = \left( \frac{m}{2\pi k_B T_{\parallel}} \right)^{1/2} \times \frac{m}{2\pi k_B T_{\perp}} \exp \left[ -\frac{m(v_{\parallel} - u)^2}{2k_B T_{\parallel}} - \frac{mv_{\perp}^2}{2k_B T_{\perp}} \right] \quad (2)$$

where  $m$  is the atomic mass and  $u$  is the local hydrodynamic velocity. Then, TW express the Boltzmann equation in spherical coordinates and apply the method of moments to obtain four differential equations coupling the density  $n$ , the hydrodynamic velocity  $u$  and the temperatures  $T_{\parallel}$  and  $T_{\perp}$  (see equations collected in table I of TW). After some algebra and neglecting small terms proportional to  $k_B T_{\parallel} / (mu^2) = 1/(2S_{\parallel}^2)$  where  $S_{\parallel}$  is the parallel speed ratio  $S_{\parallel} = u/\sqrt{2k_B T_{\parallel}/m}$  (a good approximation as  $S_{\parallel}$  becomes large in most supersonic expansions), one obtains two differential equations coupling the parallel and perpendicular temperatures:

$$\frac{dT_{\parallel}}{dz} = -2\mathcal{F} \quad (3)$$

$$\frac{dT_{\perp}}{dz} = -\frac{2T_{\perp}}{z} + \mathcal{F} \quad (4)$$

where, following BV notation, we use  $z$  to measure the distance from the nozzle.  $\mathcal{F}$  is a collision term given by:

$$\mathcal{F} = \frac{n}{2k_B u} \int g \frac{d\sigma(g)}{d\Omega} \Delta E f(\mathbf{v}_1) f(\mathbf{v}_2) d^3 \mathbf{v}_1 d^3 \mathbf{v}_2 d\Omega \quad (5)$$

In equation (5),  $\mathbf{v}_1$  and  $\mathbf{v}_2$  are the atom velocities before the collision and  $\mathbf{g} = \mathbf{v}_1 - \mathbf{v}_2$  is their relative velocity of modulus  $g$ , while  $d\sigma(g)/d\Omega$  is the differential cross-section.  $\Delta E$  is the energy transferred during one collision from the parallel degree of freedom to the perpendicular ones for the two atoms. After averaging over the azimuth describing the direction of the final relative velocity around the initial relative velocity,  $\Delta E$  is given by :

$$\langle \Delta E \rangle = \frac{m}{8} [g_\perp^2 - 2g_\parallel^2] [1 - \cos^2 \chi] \quad (6)$$

where  $\chi$  is the deflection angle.

## B. Simplification of these equations

BV have shown that the coupling term  $\mathcal{F}$  is well approximated by a linear function of  $(T_\parallel - T_\perp)$  given by  $\mathcal{F} \approx \Lambda(z) (T_\parallel - T_\perp) / 2$  with  $\Lambda(z) = 16n(z)\Omega^{(2,2)}(T_m)/(15u_\infty)$ . Here,  $\Omega^{(l,s)}(T)$  is a thermal average of the collision cross-section  $Q^{(l)}$ , both defined in reference [18] (see also Appendix A).  $T_m = (T_\parallel + 2T_\perp)/3$  is the weighted mean of the parallel and perpendicular temperatures. The hydrodynamic velocity  $u$ , in equation (5), has been replaced by its terminal value  $u_\infty = \sqrt{5k_B T_0/m}$  in the large  $S_{\parallel\infty}$  limit. Neglecting quantum effects, assuming a 12-6 Lennard-Jones potential, the  $\Omega^{(2,2)}(T)$  integral is given by:

$$\Omega^{(2,2)}(T) = 2.99 \left( \frac{2k_B T}{m} \right)^{1/2} \left( \frac{C_6}{k_B T} \right)^{1/3} \quad (7)$$

where  $C_6$  is the coefficient of the attractive term of the potential. This formula, established by BV, is valid when  $k_B T$  is small with respect to the potential well depth  $\epsilon$  (see appendix A).  $n(z)$  is related to the source density  $n_0$  and temperature  $T_0$  by  $n(z) \approx I/(u_\infty z^2)$  with the intensity  $I$  of the supersonic beam given by  $I = n_0 u_\infty z_{ref}^2$  with  $z_{ref} = 0.403 \times d$  ( $d$  is the nozzle diameter):

$$\frac{dT_\parallel}{dz} = -\Lambda(z) (T_\parallel - T_\perp) \quad (8)$$

$$\frac{dT_\perp}{dz} = -\frac{2T_\perp}{z} + \frac{\Lambda(z)}{2} (T_\parallel - T_\perp) \quad (9)$$

with  $\Lambda(z)$  given by:

$$\Lambda(z) = 3.189 \times \frac{n_0 z_{ref}^2}{u_\infty z^2} \left( \frac{2k_B T_m}{m} \right)^{1/2} \left( \frac{C_6}{k_B T_m} \right)^{1/3} \quad (10)$$

### C. Scaling and integration of these equations

When  $z$  is small, the density  $n(z)$  and the collision term  $\mathcal{F}$  are both large and the two temperatures remain equal,  $T_{\parallel} = T_{\perp} = T_m$  which verifies:

$$\frac{dT_m}{dz} = -\frac{4T_m}{3z} \quad (11)$$

giving  $T_m \propto z^{-4/3}$ . BV simplified the equations (8,9) by introducing reduced temperatures, obtained by dividing the temperatures  $T_{\parallel}$ ,  $T_{\perp}$ ,  $T_m$  by  $T_0$  and a reduced distance  $z_r = z/z_{ref}$ :

$$\frac{dT_{\parallel r}}{dz_r} = -\Xi \frac{T_{mr}^{1/6}}{z_r^2} (T_{\parallel r} - T_{\perp r}) \quad (12)$$

$$\frac{dT_{\perp r}}{dz_r} = -\frac{2T_{\perp r}}{z_r} + \Xi \frac{T_{mr}^{1/6}}{2z_r^2} (T_{\parallel r} - T_{\perp r}) \quad (13)$$

All the source parameters are condensed in the quantity  $\Xi = 0.813 \times n_0 d (C_6/k_B T_0)^{1/3}$ , which can be eliminated by a further scaling due to BV,  $z_r = \zeta \Xi^{9/11}$  and  $T_{Xr} = \tau_X \Xi^{-12/11}$  (with  $X = \parallel$  or  $\perp$ ), thus providing universal equations:

$$\frac{d\tau_{\perp}}{d\zeta} = -\frac{2\tau_{\perp}}{\zeta} + \frac{\tau_m^{1/6}(\tau_{\parallel} - \tau_{\perp})}{2\zeta^2} \quad (14)$$

$$\frac{d\tau_{\parallel}}{d\zeta} = -\frac{\tau_m^{1/6}(\tau_{\parallel} - \tau_{\perp})}{\zeta^2} \quad (15)$$

These equations have been integrated numerically by BV and, using MATLAB, we have reproduced their calculation (see figure 1 below). When  $\zeta$  is large,  $\tau_{\perp} \propto \zeta^{-1}$  while  $\tau_{\parallel}$  tends toward a limit,  $\tau_{\parallel\infty} \approx 1.15$ , from which we can express the final parallel temperature as a function of source parameters:

$$T_{\parallel\infty}/T_0 = 1.151 \times \Xi^{-12/11} \quad (16)$$

### D. Results and tests in the case of argon expansion

The tradition is to give the terminal value  $S_{\parallel\infty}$  of the parallel speed ratio rather than the terminal parallel temperature, with the relation  $T_{\parallel\infty} \approx 2.5T_0/S_{\parallel\infty}^2$ . We have written the results of TW and BV in the same form to facilitate their comparison:

$$S_{\parallel\infty} = A \left[ n_0 d (C_6/k_B T_0)^{1/3} \right]^{\delta} \quad (17)$$

TW obtained  $A = 1.413$  and  $\delta = 0.53$  by fitting the results of numerical integration of their equations written without approximations. Following the procedure we have just recalled, BV obtained  $A = 1.313$  and  $\delta = 0.545$ . In the range of practical interest, when  $5 < S_{\parallel\infty} < 50$ , these two theoretical formula never differ by more than 4% and agree when  $S_{\parallel\infty} \approx 18.9$ .

From a fit of experimental  $S_{\parallel\infty}$  values for argon, BV obtained semi-empirical values of the parameters  $A = 1.782$  and  $\delta = 0.495$ , using  $C_6(Ar - Ar)/k_B = 4.45 \times 10^{-55} \text{ K.m}^6$ . We have verified that this semi-empirical formula represents very well the  $S_{\parallel\infty}$  values for argon measured by H. D. Meyer [19] and we estimate the error bar on  $S_{\parallel\infty}$  near  $\pm 7\%$ .

### III. GENERALIZATION TO THE CASE OF A MIXTURE OF TWO MONOATOMIC GASES

#### A. Approximations used to solve the Boltzmann equation

We have two Boltzmann equations, one per species, noted  $i = 1$  for the carrier gas and  $i = 2$  for the seeded gas and the collision terms have two parts corresponding to the two collision pairs:

$$\mathbf{v}_i \cdot \mathbf{grad} [n_i(\mathbf{r})f_i(\mathbf{r}, \mathbf{v}_i)] = \Sigma_{j=1,2} \left( \frac{\partial (n_i f_i)}{\partial t} \right)_{coll} (i, j) \quad (18)$$

The densities  $f_i(\mathbf{r}, \mathbf{v}_i)$  are expressed by equation (2), with the atomic masses  $m_i$ , the temperatures  $T_{\parallel i}$  and  $T_{\perp i}$ . We assume that the hydrodynamic velocity  $u$  is the same for both species. When a heavy species is seeded in a light gas, the velocity slip effect [5, 6] is not negligible and this approximation would be bad, but we are interested in the opposite case, when the atomic mass of the seeded gas is smaller than or comparable to the atomic mass of the carrier gas. When the expansion is well in the supersonic regime, the difference of the mean velocities is negligible with respect to the thermal velocity in the moving frame (see below).

We consider the high dilution limit, when the seeded gas density  $n_2$  is considerably smaller than the carrier gas density  $n_1$ . Because  $n_2 \ll n_1$ , in the Boltzmann equation for the carrier gas distribution function  $f_1$ , we can neglect the 1 – 2 collision term. The expansion of the carrier gas is not modified by the seeded gas and the equations written above can be used to calculate the parallel and perpendicular temperatures of the carrier gas. We must simply introduce in  $\Lambda(z)$  the relevant collision integral  $\Omega_{1,1}^{(2,2)}(T)$ , where the indices designate the colliding atom pair. In the Boltzmann equation for the seeded gas  $f_2$ , we consider only the effect of 1 – 2 collisions, i.e. collisions with atoms of the carrier gas and we neglect the collisions involving two atoms of species 2. Then, we get the following equations for the temperatures of species 2:

$$\frac{dT_{\parallel 2}}{dr} = 2\mathcal{F}_{\parallel,2} \quad (19)$$

$$\frac{dT_{\perp 2}}{dr} = -\frac{2T_{\perp 2}}{r} + \mathcal{F}_{\perp 2} \quad (20)$$

with the collisional energy transfer terms given by:

$$\mathcal{F}_{X,2} = \frac{n_1}{k_B u} \int g \frac{d\sigma_{1,2}(g)}{d\Omega} \Delta E_{X,2} f_1(\mathbf{v}_1) f_2(\mathbf{v}_2) d^3 \mathbf{v}_1 d^3 \mathbf{v}_2 d\Omega \quad (21)$$

where  $\Delta E_{X,2}$  ( $X = \parallel$  or  $\perp$ ) measures the parallel or perpendicular energy gained by atom 2 during the collision with atom 1. We can express  $\Delta E_{X,2}$  with the parallel and perpendicular components of the center of mass velocity and of the relative velocity. However, when the four temperatures are not equal, the product  $f_1(\mathbf{v}_1) f_2(\mathbf{v}_2)$  has not a simple form when expressed with these velocities and we have not been able to calculate exactly the resulting integrals. Therefore, to get an analytic result for  $\mathcal{F}_{X,2}$ , we have used the following approximation. When the collision energy is small, the cross-sections  $Q_{1,2}^{(l)}(g)$  behave like  $g^{-2/3}$  and the

products  $gQ_{1,2}^{(l)}(g)$  vary slowly with  $g$ , like  $g^{1/3}$ . We take these products  $gd\sigma_{1,2}(g)/d\Omega$  out of the integrals over  $\mathbf{v}_1$  and  $\mathbf{v}_2$  to get:

$$\mathcal{F}_{X,2} \approx \frac{n_1}{k_B u_\infty} \int \langle g \frac{d\sigma_{1,2}(g)}{d\Omega} \rangle d\Omega \int \Delta E_{X,2} f_1(\mathbf{v}_1) f_2(\mathbf{v}_2) d^3\mathbf{v}_1 d^3\mathbf{v}_2 \quad (22)$$

The calculation of this integral is described in appendix B.

## B. Coupled equations describing the temperatures of the two gases

The coupled equations for the carrier gas  $i = 1$  have been established in part II (equations (8) and (9)) where  $T_X$  must be replaced by  $T_{X1}$ . In the differential equations for the temperatures of the seeded gas  $i = 2$ , we have quantities similar to  $\Lambda(z)$  but involving the  $\Omega_{1,2}^{(l,2)}(T_m)$  integrals with  $l = 1$  and  $2$ . By introducing two dimensionless ratios  $\rho_s$  and  $\rho_o$ , we can express these quantities as a function of  $\Omega_{1,1}^{(2,2)}(T_m)$ .  $\rho_s$  is the ratio of  $\Omega_{i,j}^{(2,2)}$  collision integrals differing by the species of the second collision partner and its value is deduced from equation (7):

$$\rho_s = \frac{\Omega_{1,2}^{(2,2)}}{\Omega_{1,1}^{(2,2)}} = \left[ \frac{C_6(1,2)}{C_6(1,1)} \right]^{1/3} \times \left[ \frac{m_1 + m_2}{2m_2} \right]^{1/2} \quad (23)$$

$\rho_s$  depends slowly on the  $C_6$  ratio and more rapidly on the mass ratio.  $\rho_o$  is the ratio of angle-averaged cross-sections of orders  $l = 1$  and  $l = 2$ , defined by  $\rho_o = \Omega_{1,2}^{(1,2)}/\Omega_{1,2}^{(2,2)} = 1.32$  (see Appendix A and our previous paper [1]).

$$\begin{aligned} \frac{dT_{\perp 2}}{dz} &= -\frac{2T_{\perp 2}}{z} + \Lambda(z)\rho_s \frac{m_1}{M} [T_{\parallel,av} - T_{\perp,av}] \\ &\quad - 4\Lambda(z)\rho_s\rho_o \frac{\mu}{M} [T_{\perp 2} - T_{\perp 1}] \end{aligned} \quad (24)$$

$$\begin{aligned} \frac{dT_{\parallel 2}}{dz} &= -2\Lambda(z)\rho_s \frac{m_1}{M} [T_{\parallel,av} - T_{\perp,av}] \\ &\quad - 4\Lambda(z)\rho_s\rho_o \frac{\mu}{M} [T_{\parallel 2} - T_{\parallel 1}] \end{aligned} \quad (25)$$

$\Lambda(z)$  being given by equation (10) and  $T_{X,av}$  being defined by:

$$T_{X,av} = \beta T_{X1} + \alpha T_{X2} \quad (26)$$

with  $\alpha = m_1/M$ ,  $\beta = m_2/M$ ,  $M = m_1 + m_2$  and  $\mu = m_1 m_2 / (m_1 + m_2)$ . One should remark that in  $T_{X,av}$ , the weight of  $T_{X1}$  is  $\beta = m_2/M$  and the weight of  $T_{X2}$  is  $\alpha = m_1/M$ . We proceed as in part I.C and we get two equations verified by  $\tau_{\parallel 2}$  and  $\tau_{\perp 2}$ :

$$\begin{aligned} \frac{d\tau_{\perp 2}}{d\zeta} &= -\frac{2\tau_{\perp 2}}{\zeta} + \frac{\rho_s \tau_m^{1/6}}{\zeta^2} \times \frac{m_1}{M} (\tau_{\parallel,av} - \tau_{\perp,av}) \\ &\quad - \frac{4\rho_s \rho_o \tau_m^{1/6}}{\zeta^2} \times \frac{\mu}{M} (\tau_{\perp 2} - \tau_{\perp 1}) \end{aligned} \quad (27)$$

$$\begin{aligned} \frac{d\tau_{\parallel 2}}{d\zeta} = & -\frac{2\rho_s\tau_m^{1/6}}{\zeta^2} \times \frac{m_1}{M} (\tau_{\parallel,av} - \tau_{\perp,av}) \\ & - \frac{4\rho_s\rho_o\tau_m^{1/6}}{\zeta^2} \times \frac{\mu}{M} (\tau_{\parallel 2} - \tau_{\parallel 1}) \end{aligned} \quad (28)$$

A simple test of the coherence of our calculations is to consider that the two species have the same masses ( $m_1 = m_2$ ) and the same collision cross-sections ( $\rho_s = 1$ ). We then expect that the parallel and perpendicular temperatures are independent of the species ( $\tau_{X1} = \tau_{X2}$  for all  $\zeta$  values) and this property is well verified.

Using MATLAB, we have integrated the equations (27,28) and the results are represented in figure 1. At the end of the expansion, the parallel and perpendicular temperatures of the seeded gas are intermediate between the same quantities for the carrier gas. In particular, the terminal value of the parallel temperature ratio  $\tau_{\parallel 2,\infty}/\tau_{\parallel 1,\infty} = T_{\parallel 2,\infty}/T_{\parallel 1,\infty}$  can be substantially lower than 1. The absolute minimum value for this temperature ratio is reached when the right-hand side of equation (25) vanishes. Assuming that the perpendicular temperatures are both negligible, we get the minimum possible value of the ratio  $T_{\parallel 2,\infty}/T_{\parallel 1,\infty}$ :

$$\text{Min} \left( \frac{T_{\parallel 2,\infty}}{T_{\parallel 1,\infty}} \right) = \frac{m_2\rho_o}{m_1 + 2m_2\rho_o} \quad (29)$$

This limiting value would be reached if the ratio  $\rho_s$  tends toward infinity. We have plotted in figure 2 the terminal value of the ratio  $T_{\parallel 2,\infty}/T_{\parallel 1,\infty}$  for various values of the ratio  $\rho_s$ , as a function of the mass ratio  $m_2/m_1$ . When the mass ratio  $m_2/m_1$  is very small, the parallel temperature of the seeded gas can be considerably smaller than the one of the carrier gas. We can make some surprising predictions:

- In the case of molecular hydrogen  $\text{H}_2$  seeded in argon, using to calculate the Ar- $\text{H}_2$   $C_6$  coefficient the combination rule and the data of Kramer and Herschbach [20], we get  $\rho_s = 2.48$  from which we predict a temperature ratio  $T_{\parallel 2,\infty}/T_{\parallel 1,\infty} = 0.16$ , a quite large effect!
- for a beam of potassium seeded in argon, the two atomic masses are almost equal and, with the  $C_6$  from reference [26], we get  $\rho_s = 1.67$ . We predict a temperature ratio  $T_{\parallel 2,\infty}/T_{\parallel 1,\infty} = 0.77$ , already smaller than 1.
- for a beam of sodium seeded in neon, we calculate in the same way  $\rho_s = 1.85$ , (the large  $C_6$  ratio overcompensates the effect of the mass ratio  $m_2/m_1 = 1.14$ ) and we predict a temperature ratio  $T_{\parallel 2,\infty}/T_{\parallel 1,\infty} = 0.77$ , also smaller than 1. This is not a large effect, but this result, with  $T_{\parallel 2,\infty} < T_{\parallel 1,\infty}$  while  $m_2 > m_1$ , is contrary to the common belief recalled in the introduction.

### C. Discussion

In addition to the approximations already done by Beijerinck and Verster, we have neglected the velocity slip, which has been studied in particular by Anderson [5] and by Miller and Andres [6]. Equations (2.37,2.38) of Miller [13]) give the velocity difference  $u_{2,\infty} - u_{1,\infty}$ , which can be written with our notations and in the high dilution limit:



$$\frac{u_{2,\infty} - u_{1,\infty}}{u_{1,\infty}} \approx 0.59 \left[ \frac{\sqrt{\mu m_1}}{|m_1 - m_2|} n_0 d (C_6/k_B T_0)^{1/3} \right]^{-1.07} \quad (30)$$

The  $\Omega_{1,2}^{(1,1)}$  integral, which appears in these equations, is evaluated in Appendix A. The physically important quantity is the ratio of this velocity difference ( $u_{2,\infty} - u_{1,\infty}$ ) divided by the parallel thermal velocity of atom 1, namely  $\sqrt{2k_B T_{\parallel 1}/m_1}$ . Using equation (17) in the TW form and approximating the 1.07 exponent by  $2 \times 0.53$ , we get:

$$\frac{u_{2,\infty} - u_{1,\infty}}{\sqrt{2k_B T_{\parallel 1}/m_1}} \approx \frac{0.84}{S_{\parallel 1\infty}} \left[ \frac{(m_1 + m_2)(m_1 - m_2)^2}{m_1^2 m_2} \right]^{0.53} \quad (31)$$

If the terminal parallel speed ratio  $S_{\parallel 1\infty}$  is large, the velocity slip is a small fraction of the parallel thermal velocity of atom 1, provided that the masses  $m_1$  and  $m_2$  are not extremely different. In this case, neglecting the velocity slip is an excellent approximation.

In equation (21), we have also treated the products  $gQ_{1,2}^{(l)}(g)$  as constant. Takahashi and Teshima were able to calculate numerically these integrals when they studied the case of a heavy gas seeded in a light gas [16]. Using their technique, it would be possible to test the accuracy of our approximation.

Monte Carlo simulation can also be used to simulate flows of gases and gas mixtures. The Direct Simulation Monte Carlo method described by G. A. Bird in his book [22] is the best method and it has been used very early to simulate supersonic expansions [15, 23]. This method requires much computation in the high dilution case [21] and P. A. Skovorodko has used the Test Particle Monte Carlo method to simulate the expansion of gas mixtures. This method also involves an approximation, the use of Maxwell type interaction potential. He has simulated our lithium seeded in argon expansion and his results support our calculations, at least at the qualitative level [24]. In his simulations, P. A. Skovorodko has found that the distribution of the perpendicular velocity of lithium differs very much from a Maxwellian distribution and is almost perfectly exponential. The fact that the velocity distribution of the perpendicular degree of freedom cannot be Maxwellian was analyzed in detail by Beijerinck and co-workers who suggested to call blistering this effect [11, 25]. This effect cannot be taken into account by the theory described in the present paper as the assumption of an elliptic Maxwellian velocity distribution is the starting point of the solution of Boltzmann equation.

#### IV. COMPARISON WITH EXPERIMENTAL RESULTS

In this part, we first describe briefly the previous experimental cases in which the light gas parallel temperature has been found lower than the carrier gas parallel temperature. Then, we describe our experiment with a beam of lithium seeded in argon and a new set of temperature measurements.

##### A. Sodium in seeded in argon

A beam of sodium seeded in argon was built by D. Pritchard and coworkers [33] with a source temperature near 1000 K, an argon pressure up to  $p_0 = 3$  bars and a nozzle diameter

$d = 70 \text{ } \mu\text{m}$ . In a particular experiment [34], the mean velocity was measured,  $u = 1040 \pm 2 \text{ m/s}$  corresponding to  $T_0 = 1039 \text{ K}$ , and the rms velocity width, deduced from the atomic diffraction pattern, was found equal to  $3.7 \pm 0.4\%$ , corresponding to  $T_{\parallel 2\infty} = 4.1 \pm 0.9 \text{ K}$ . Assuming that this experiment was made with the largest pressure quoted in [33], we calculate the argon parallel temperature  $T_{\parallel 1} = 7.7 \pm 1.1 \text{ K}$ , from which we deduce the parallel temperature ratio  $T_{\parallel 2\infty}/T_{\parallel 1\infty} = 0.53 \pm 0.19$ . This value is in good agreement with our theoretical result is  $T_{\parallel 2\infty}/T_{\parallel 1\infty} = 0.66$ , deduced from the value of  $\rho_s = 1.67$  (obtained with the  $C_6$  values from reference [26]).

## B. Atomic oxygen seeded in argon

In 2000, Campargue and co-workers [2] operated and characterized a beam of atomic oxygen seeded in argon produced by a laser plasma source. The oxygen parallel temperature was roughly half the argon parallel temperature (see figure 10 of reference [2]). The numerical model described in this paper supports the experimental results. Let us compare this result with our theory. Using the combination rule of Kramer and Herschbach [20] and data for oxygen from reference [27], we calculate the oxygen-argon  $C_6$  coefficient  $C_6(O - Ar) = 34$  atomic units and  $\rho_s = 1.06$ . Our theory then predicts a temperature ratio  $T_{\parallel 2,\infty}/T_{\parallel 1,\infty} = 0.76$ , substantially larger than the experimental value near 0.5. This discrepancy is probably due to the fact that, because of the very high source temperature close to  $10^4 \text{ K}$ , the terminal parallel temperatures are considerably higher in this case than for usual beam experiments, in the  $70 - 130 \text{ K}$  range for oxygen and  $220 - 150 \text{ K}$  range for argon. For such terminal temperatures, we cannot expect the low temperature approximations of the  $\Omega^{(l,s)}(T)$  integrals to be valid.

## C. Lithium seeded in argon

### 1. The beam source

Our beam [28] is inspired by the design used by Broyer, Dugourd and co-workers to produce lithium clusters [29]. The temperatures used in our experiment are usually equal to  $973 \text{ K}$  for the back part of the oven, corresponding to a lithium vapor pressure of  $0.55$  millibar and to  $1073 \text{ K}$  for the front part. The nozzle is a hole of  $200 \text{ } \mu\text{m}$  diameter drilled in a stainless steel  $0.3 \text{ mm}$  thick wall. The argon gas (from Air Liquide,  $99.999\%$  stated purity) is further purified by a purifying cartridge also from Air Liquide and its pressure can be varied from  $150$  to  $800$  millibar, limited by the throughput of our oil diffusion pump (Varian VHS400 with a  $8000 \text{ l/s}$  pumping speed) backed by a Leybold D65B roughing pump ( $65 \text{ m}^3/\text{hour}$  pumping speed). For a source pressure  $p_0 = 300$  millibar, the pressure at the diffusion pump is  $8 \times 10^{-4}$  millibar. We use a skimmer from Beam Dynamics with  $0.97 \text{ mm}$  aperture at a  $20 \text{ mm}$  distance from the nozzle. After the skimmer, the lithium beam is in a separate vacuum tank pumped by an oil diffusion pump (Varian VHS6 with a  $2400 \text{ l/s}$  pumping speed) fitted with a water cooled baffle. Under beam operation, when  $p_0 = 300$  millibar, the pressure in this chamber is  $3 \times 10^{-6}$  millibar.

## 2. Doppler measurement of the parallel and perpendicular velocity distribution

In the center of the second vacuum tank, i.e. 225 mm after the skimmer, the lithium beam is crossed by two laser beams *A* and *B*. The angle between the atomic beam and the laser beams are  $\theta_A = 47.9 \pm 0.5^\circ$  and  $\theta_B \approx 90^\circ$ . The first order Doppler effect is sensitive only to the projection  $v_p$  of the velocity on the laser beam axis. For a laser beam making the angle  $\theta$  with the axis of the atomic beam, the distribution of  $v_p$  is deduced from equation (2):

$$f(v_p) = \left( \frac{m}{2\pi k_B T(\theta)} \right)^{1/2} \exp \left[ -\frac{m(v_p - u \cos \theta)^2}{2k_B T(\theta)} \right] \quad (32)$$

with  $T(\theta) = T_{\parallel} \cos^2 \theta + T_{\perp} \sin^2 \theta$ . The distribution  $f(v_p)$  is centered at  $v_p = u \cos \theta$  and its width is characterized by a weighted mean of the parallel and perpendicular temperatures. The fluorescence intensity as a function of the laser frequency reflects the velocity distribution if the natural width of the excited transition is negligible with respect to the Doppler width and if saturation broadening of the transition as well as laser frequency jitter are both negligible.

The laser excites successively the hyperfine components of the  $^2S_{1/2} - ^2P_{3/2}$  resonance transition of lithium at 671 nm [30]. The very small hyperfine splittings of the upper state can be neglected. The ground state has two hyperfine components  $F = 1$  and  $F = 2$ , with a splitting equal to 803.5 MHz. The natural width of the transition is  $\Gamma/2\pi = 5.87$  MHz [31] and we use laser power density of the order of  $10^{-2}$  mW/cm<sup>2</sup>, corresponding to a saturation parameter  $s \approx 5 \times 10^{-3}$  and a negligible broadening of the excitation line. Our single frequency cw dye laser pumped by an argon ion laser has a linewidth of the order of 1 MHz, thanks to the Hänsch-Couillaud [32] frequency stabilization technique.

Figure 3 shows such a laser induced fluorescence spectrum: for beam *A*, the Doppler full widths are of the order of 200 MHz and the natural width as well as the laser linewidth are negligible. During our experiment, we have also recorded a saturated absorption spectrum in a heat pipe oven: this signal provides Doppler-free peaks which are useful if one wants to measure accurately the mean velocity  $u$  of the atomic beam, because, in some experiments, the laser beam *B* is not exactly perpendicular to the atomic beam.

## 3. Experimental results

From the analysis of the fluorescence signals, we can deduce the beam mean velocity  $u = 1010 \pm 10$  m/s, slightly less than the value deduced from the source temperature,  $u_{\infty} = \sqrt{5k_B T_0/m} = 1056$  m/s. The width of the *B* peaks is related to the perpendicular temperature of the beam but we think that the perpendicular temperature  $T_{\perp}$  thus deduced is overestimated because our detector is not observing only one streamline. The width of the *A* peaks provide the weighted mean  $T(\theta)$  of the temperatures, from which we can deduce the parallel temperature. As we think that our measurement may overestimate the perpendicular temperature, we have neglected the contribution of the perpendicular temperature when extracting the parallel temperature from  $T(\theta)$ , i.e. we have used:

$$T_{\parallel} = T(\theta) / \cos^2 \theta \quad (33)$$

so that we get an upper limit of the parallel temperature  $T_{\parallel}$ . In table I, we have also given the fluorescence signal intensity which gives an idea of the intensity of the lithium beam.

Source pressure (mbar)	$T_{\parallel 2}(K)$	$T_{\perp 2}(mK)$	Fluorescence signal(a.u.)
200	10.1	493	8.5
267	7.6	514	7.9
333	6.6	497	7.0
400	6.0	488	5.8
467	6.1	546	6.6
534	6.0	593	5.0
600	5.3	550	5.6

This intensity decreases when the argon pressure increases. This behavior is probably due to the interaction of the beam with the residual gas near the skimmer.

The measured parallel temperature is plotted as a function of argon pressure in figure 4. The full curve is a plot of our results with the ratio  $T_{\parallel 2}/T_{\parallel 1}$  taken equal to its predicted value 0.38. The dashed curve is obtained by fitting the value of this ratio  $T_{\parallel 2}/T_{\parallel 1}$  to the four data points with an argon pressures smaller than 400 millibar: the fitted value is equal to 0.31.  $T_{\parallel 1}$  is related to the source parameters by equation (17), using the semi-empirical coefficients of BV. For larger pressures, the parallel temperature remains constant while theory predicts that it should still decrease. We think that this discrepancy may be due to the interaction of the beam with the residual gas discussed above.

Another explanation could be cluster formation in the expansion. Following the results of Hagena [35] further discussed by Beijerinck and Verster [11], for an argon beam, a safe upper limit to prevent cluster formation is to keep the quantity  $p_0 d^{0.88} T_0^{-2.3} < 4.9 \times 10^{-7} \text{ mbar m}^{0.88} \text{ K}^{-2.3}$ . At our largest source pressure  $p_0 = 600 \text{ mbar}$ , the quantity  $p_0 d^{0.88} T_0^{-2.3} = 3.6 \times 10^{-8} \text{ mbar m}^{0.88} \text{ K}^{-2.3}$  is well below this upper limit. As the LiAr molecule is considerably less bound than the  $\text{Ar}_2$  molecule [39, 40] and as the lithium concentration is very small, we think that the threshold for the formation of mixed clusters is also not reached.

## V. SUMMARY

The knowledge concerning the terminal parallel temperatures produced by supersonic expansions of a mixture of monoatomic gases has been developed for many years and the case of heavy atom seeded in a light carrier gas, which has been subject of almost all the studies, is extremely well understood. The opposite case (a light gas seeded in an heavier carrier gas) had been rarely studied, an exception being the work of Campargue and co-workers [2] in 2000. This opposite case might seem of limited interest but some experiments (for instance, atom interferometry) require a rather slow atomic beam with a small velocity dispersion: in this case, seeding a light gas in an heavier carrier gas is the most natural solution.

In the present paper, we have developed a theoretical analysis by making a slight extension of the theoretical works of Toennies and Winkelmann [10] and of Beijerinck and Verster [11]. With some new approximations, we obtain an analytic treatment of the problem, valid in the high dilution limit. We thus rationalize the surprising experimental result we had observed after Campargue and co-workers [2]: the parallel temperature of the seeded gas can be lower than the same quantity for the carrier gas. We have found that this effect depends on two

quantities, the ratio  $\rho_s$  of cross-sections for the two gases, defined by equation (23), and the ratio of the atomic masses  $m_2/m_1$ . Finally, the physical basis of this ultra cooling effect is not mysterious and we have explained it in the introduction.

In a final part, we have discussed the available experimental evidences of this effect, due to other groups [2, 33, 34] and we have described our experiment with a beam of lithium seeded in argon. We have presented a set of experimental data considerably larger than in our first study [1]. The agreement between our theoretical prediction and experiments can be considered as good in the cases of sodium and lithium seeded in argon. The agreement is less good for the argon-oxygen beam but we understand why it is so.

We think that the ultra cooling effect described here is now well established and some further studies would be very interesting. First of all, it should be easy to observe this effect in several other experimental cases, some of them being discussed in part III.B: a particularly striking case would be to seed molecular hydrogen in argon or even heavier rare gases. From the theoretical point of view, it is interesting to investigate this effect by other methods and Monte Carlo simulation, which has been already applied to this problem by P. A. Skovorodko [24], is particularly well suited as the approximations needed to solve Boltzmann equation can be removed.

## VI. ACKNOWLEDGEMENTS

We thank J.P. Toennies, H. C. W. Beijerinck, U. Buck and P. A. Skovorodko for helpful discussions. We also thank Ph. Dugourd and M. Broyer for advice concerning the design of the oven of our lithium supersonic beam, J. Schmiedmayer for advice concerning the use of LD688 dye as well as R. Delhuille, L. Jozefowski and C. Champenois for their important contributions to the construction of our experimental setup. We thank CNRS-SPM, Région Midi Pyrénées, IRSAMC and Université P. Sabatier for financial support.

## VII. APPENDIX A: WEIGHTED CROSS-SECTIONS; THEIR DEFINITION AND CALCULATION OF THEIR TEMPERATURE DEPENDENCE

### A. Definitions

We consider the collision between two atoms of species  $i$  and  $j$  with a relative velocity  $g$  and a reduced mass  $\mu = m_i m_j / (m_i + m_j)$ . The definitions and many results are taken from the book Molecular theory of gases and liquids, by Hirschfelder, Curtiss and Bird [18]. Starting from the differential cross-section  $d\sigma_{i,j}(g)/d\Omega$ , the angle-weighted cross-sections  $Q_{i,j}^{(l)}(g)$  are defined by (equation 8.2-2 of [18]) :

$$Q_{i,j}^{(l)}(g) = \int \frac{d\sigma_{i,j}(g)}{d\Omega} (1 - \cos^l \chi) d\Omega \quad (34)$$

where  $\chi$  is the deflection angle. In classical mechanics, the deflection angle  $\chi$  is a function of the impact parameter  $b$  and the relative velocity  $g$ .  $Q_{i,j}^{(l)}(g)$  is then given by:

$$Q_{i,j}^{(l)}(g) = \int (1 - \cos^l \chi) 2\pi b db \quad (35)$$

The thermal averages  $\Omega_{i,j}^{(l,s)}(T)$  are given by equation (8.2-3) of reference [18]:

$$\Omega_{i,j}^{(l,s)}(T) = \sqrt{k_B T / (2\pi\mu)} \int_0^\infty Q_{i,j}^{(l)}(g) \gamma^{2s+3} \exp(-\gamma^2) d\gamma \quad (36)$$

with  $\gamma^2 = \mu g^2 / (2k_B T)$ . Three circumstances contribute to make classical mechanics a good approximation in the experimental cases considered here:

- the quantum character of the interaction between two identical atoms of mass  $m$  is measured by the quantum parameter  $\eta = \hbar^2 / (m\sigma^2\epsilon)$  introduced by Stwalley and Nosanow [36] (see also De Boer and Lunbeck [37]) where  $\epsilon$  is the potential well depth and  $\sigma$  the core radius. A large  $\eta$  value indicates a highly quantum behavior while a small one corresponds to a quasi-classical behavior.  $^4\text{He}$  dimer is highly quantum with  $\eta \approx 0.18$  [36], while  $\text{Ar}$  dimer [40] with  $\eta \approx 0.75 \times 10^{-3}$  and  $^7\text{Li} - \text{Ar}$  [39] with  $\eta \approx 6.6 \times 10^{-3}$  have a weak quantum character.
- the differential cross-section presents several types of quantum effects. These effects are largely reduced by the angle average following equation (34) and further reduced by the thermal average following equation (36).
- a quantum effect which survives these averages is the behavior of the cross-section at very low energy. This is the quantum threshold regime, which extends up to an energy of the order of  $\hbar^3 \mu^{-3/2} C_6^{-1/2}$  for an potential with a  $C_6/r^6$  long range, following Julienne and Mies [38]. This effect explains the very large helium-helium cross-section at low energy [10]. For argon-argon and lithium-argon collisions, we find that this regime could be observed for temperatures of the order of  $10^{-2}$  and  $2 \times 10^{-2}$  Kelvin respectively, well below the lowest temperatures obtained in argon expansions, of the order of 1 Kelvin [11, 19].

## B. Calculations with a Lennard-Jones 12 – 6 potential

We consider an interaction potential of the 12 – 6 Lennard-Jones type:

$$V(r) = \frac{C_{12}}{r^{12}} - \frac{C_6}{r^6} = 4\epsilon \left[ \frac{\sigma^{12}}{r^{12}} - \frac{\sigma^6}{r^6} \right] \quad (37)$$

using the usual reduced quantities (see paragraph 8.2 of [18]). In a first step, we have calculated the deflection function  $\chi(b)$  as a function of the reduced energy  $E^* = \mu g^2 / (2\epsilon)$ , by numerical integration. Our calculation reproduces well the analytic deflection function of BV for  $E^* \leq 0.1$  (see appendix A of [11]).

We have then calculated the  $Q^{(l)}(g)$  cross-sections with  $l = 1$  and  $l = 2$  as a function of  $E^*$ . In the low-energy range,  $E^* \ll 1$ , these two cross-sections are well approximated by an  $(E^*)^{-1/3}$  behavior and, to make this behavior very clear, we have plotted in figure 5 the variation of  $Q^{(l)}(g)E^{*1/3}$  as a function of  $E^*$ . At low energy, our calculation presents a small numerical noise associated to the orbiting singularity. We have not tried to reduce this noise by introducing some analytic approximations of the function  $\chi(b)$  near this singularity.

When  $E^* \rightarrow 0$ , we get:

$$Q^{(1)}(g) \approx (7.81 \pm 0.01) \sigma^2 E^{*-1/3} \quad (38)$$

and

$$Q^{(2)}(g) \approx (5.95 \pm 0.01)\sigma^2 E^{*-1/3} \quad (39)$$

Then, we have calculated numerically the  $\Omega^{(l,s)}$  integrals as a function of the reduced temperature  $T^* = k_B T / \epsilon$  and we have verified their low energy limits analytically (this is easy as the integral in equation (36) can be expressed by a Gamma function). The various  $\Omega^{(l,s)}(T)$  take a form analogous to equation (7):

$$\Omega^{(2,2)}(T) = C^{(l,s)}(T^*) \left( \frac{k_B T}{\mu} \right)^{1/2} \left( \frac{C_6}{k_B T} \right)^{1/3} \quad (40)$$

We have plotted in figure 6 the variations of three functions  $C^{(l,s)}(T^*)$ . We are mostly interested in their low-temperature limits, which are necessary for our calculations. We thus obtain  $C^{(2,2)}(0) = 3.00$ , in excellent agreement with the value 2.99 obtained by BV [11],  $C^{(1,2)}(0) = 3.94$  and  $C^{(1,1)}(0) = 1.48$ . We also get the value of the ratio  $\rho_o = C^{(1,2)}(0)/C^{(2,2)}(0) = 1.312 \pm 0.004$ , also in very good agreement with the value  $\rho_o = 1.32$  deduced from the analytic deflection function of BV [11].

## VIII. APPENDIX B: CALCULATION OF $\mathbf{F}_{\parallel,2}$ AND $\mathbf{F}_{\perp,2}$

We must calculate:

$$\mathcal{F}_{X,2} \approx \frac{n_1}{k_B u_\infty} \int \langle g \frac{d\sigma(g)}{d\Omega} \rangle d\Omega \int \Delta E_{X,2} f_1(\mathbf{v}_1) f_2(\mathbf{v}_2) d^3 \mathbf{v}_1 d^3 \mathbf{v}_2 d\Omega \quad (41)$$

with  $X = \parallel$  and  $\perp$ . We introduce the center of mass velocity  $\mathbf{v}_{cm}$

$$\mathbf{v}_{cm} = \alpha \mathbf{v}_1 + \beta \mathbf{v}_2 \quad (42)$$

with  $\alpha = m_1/M$ ,  $\beta = m_2/M$  and  $M = m_1 + m_2$ . The relative velocity before the collision is  $\mathbf{g} = \mathbf{v}_1 - \mathbf{v}_2$  and after the collision is  $\mathbf{g}_f$ . The deflection angle noted  $\chi$  is the angle between  $\mathbf{g}$  and  $\mathbf{g}_f$ , which have the same modulus. We must also introduce the azimuth  $\varphi$  measuring the orientation in space of the plane  $\mathbf{g}, \mathbf{g}_f$ . This azimuth  $\varphi$  is equally probable in the  $0 \leq \varphi < 2\pi$  range. The final velocity of atom 2 is given by:

$$\mathbf{v}_{2f} = \alpha \mathbf{v}_1 + \beta \mathbf{v}_2 - \alpha \mathbf{g}_f \quad (43)$$

We express its parallel and perpendicular components as a function of the initial velocities, of the relative velocity and of the various angles and we want to calculate:

$$\Delta E_{2X} = \frac{m_2}{2} (\mathbf{v}_{2fX}^2 - \mathbf{v}_{2X}^2) \quad (44)$$

We then integrate these quantities over the angles and over the velocities  $\mathbf{v}_1$  and  $\mathbf{v}_2$  with the normalized functions  $f_1(\mathbf{v}_1) f_2(\mathbf{v}_2)$ . All the terms involve double products of the type  $v_{iX} v_{jY}$ , where  $i, j$  stands for atom indices 1, 2 and  $X, Y$  for  $\parallel$  or  $\perp$ . After integration, all these products vanish, excepted the ones with  $i = j$  and  $X = Y$  and their values are simply

related to the temperature associated to this atom and this degree of freedom:

$$\begin{aligned}\Delta E_{2\parallel} = & \frac{m_2}{2} \left[ \frac{k_B T_{\parallel 1}}{m_1} \alpha^2 (1 - \cos \chi)^2 - \frac{k_B T_{\parallel 2}}{m_2} (\alpha^2 \sin^2 \chi + 2\alpha\beta (1 - \cos \chi)) \right. \\ & \left. + \left( \frac{k_B T_{\perp 1}}{m_1} + \frac{k_B T_{\perp 2}}{m_2} \right) \alpha^2 \sin^2 \chi \right]\end{aligned}\quad (45)$$

$$\begin{aligned}\Delta E_{2\perp} = & \frac{m_2}{2} \left[ \left( \frac{k_B T_{\parallel 1}}{m_1} + \frac{k_B T_{\parallel 2}}{m_2} \right) \alpha^2 \sin^2 \chi + \frac{k_B T_{\perp 1}}{m_1} \alpha^2 (3 + \cos^2 \chi - 4 \cos \chi) \right. \\ & \left. - \frac{k_B T_{\perp 2}}{m_2} (4\alpha\beta (1 - \cos \chi) + \alpha^2 \sin^2 \chi) \right]\end{aligned}\quad (46)$$

Finally we integrate over  $\chi$ . The integrals involve the angular weights  $(1 - \cos^l \chi)$  with  $l = 1$  and 2 only, i.e. they involve only  $Q_{1,2}^{(1)}$  and  $Q_{1,2}^{(2)}$  defined by equation (34). There was no terms involving  $l = 1$  terms in the pure gas case. This new feature is due to the fact that the forward-backward symmetry existing in the pure gas case is now broken by the different masses of the two colliding atoms and by the fact that we calculate the energy transfer for atom 2 only.

We have made an approximation by considering  $gQ_{1,2}^{(l)}(g)$  as independent of  $g$  and we must fix its value. To be coherent with the pure gas case, we have made the same approximation in the pure gas case and we have identified the two values of  $\Lambda(z)$ :

$$\langle gQ_{1,2}^{(l)}(g) \rangle = \frac{32}{15} \Omega_{1,2}^{(l,2)}(T_m) \quad (47)$$

As  $\Omega_{1,2}^{(l,2)}(T_m)$  varies very slowly with  $T_m$ , like  $T_m^{1/6}$ , the exact choice for  $T_m$  is not important and we have always used  $T_m = (T_{\parallel 1} + 2T_{\perp 1})/3$ .



- 
- [1] A. Miffre, M. Jacquy, M. Büchner, G. Trénec and J. Vigué, accepted for publication in Phys. Rev. A, [ArXiv.org/abs/physics/0401019](https://arxiv.org/abs/physics/0401019)
  - [2] A. Lebehot, J. Kurzyna, V. Lago, M. Dudeck, and R. Campargue in "Atomic and Molecular Beams, The State of the Art 2000", R. Campargue Ed. (Springer) p 237 (2001)
  - [3] R. Campargue, J. Phys. Chem. **88**, 4466 (1984)
  - [4] R. Campargue, A. Lebehot, J. C. Lemonnier, and D. Marette (RGD - 12, Charlottesville, Va., USA) in Rarefied Gas Dynamics, S. S. Fisher Ed., (AIAA, New York) Vol. II, 823 (1981)
  - [5] J. B. Anderson, Entropie **18**, 33 (1967)
  - [6] D. R. Miller and R. P. Andres, in Rarefied Gas Dynamics, L. Trilling and H. Y. Wachman eds. (Academic Press, New York) vol 2, p. 1385 (1969)
  - [7] J. B. Anderson and J. B. Fenn, Phys. Fluids **8**, 780 (1965)
  - [8] B. B. Hamel and D. R. Willis, Phys. Fluids, **9**, 8289 (1966)
  - [9] E. L. Knuth and S. S. Fisher, J. Chem. Phys. **48**, 1674 (1968)
  - [10] J. P. Toennies and K. Winkelmann, J. Chem. Phys. **66**, 3965 (1977)
  - [11] H. C. W. Beijerinck and N. F. Verster, Physica **111C**, 327 (1981)
  - [12] A. L. Cooper and C. K. Bienkowski (RGD-5, Oxford, UK, 1966) in Rarefied Gas Dynamics, C. L. Brundin Ed., (Academic Press, New York) Vol. I, 861 (1967)
  - [13] D. R. Miller, in Atomic and molecular beam methods, G. Scoles ed., (Oxford University Press), p. 14 (1988)
  - [14] P. Raghuraman, P. Davidovits, and J. B. Anderson, Rarefied Gas Dynamics 10th Symposium, Aspen, 1976 (J. L. Potter editor, AIAA) Progress in Astronautics and Aeronautics, **51-1** 79 (1977)
  - [15] R. J. Cattolica, R. J. Gallagher, J. B. Anderson, and L. Talbot, AIAA Journal, **17**, 344 (1979)
  - [16] N. Takahashi and K. Teshima, in Rarefied Gas Dynamics 14th Symposium, H. Oguchi ed. (University of Tokyo Press) vol 2, p. 703 (1984)
  - [17] A. Chesneau and R. Campargue (RGD-13, Novosibirsk, USSR) in Rarefied Gas Dynamics, O.N. Belotserkovskii et al. Eds. (Plenum, New York) p. 879 (1985)
  - [18] J. O. Hirschfelder, C. F. Curtiss and R. B. Bird, Molecular theory of liquids, (Wiley, New York, 1954)
  - [19] H. D. Meyer, MPI für Strömungsforschung, Bericht 5 (Göttingen, 1978)
  - [20] H. L. Kramer and D. R. Herschbach, J. Chem. Phys. **53**, 2792 (1970)
  - [21] P. A. Skovorodko, private communication (January 2004)
  - [22] G. A. Bird, Molecular dynamics and the direct simulation of gas flows, Oxford University Press, Oxford (1994)
  - [23] G. A. Bird, AIAA Journal, **8**, 1998 (1970)
  - [24] P. A. Skovorodko, abstract submitted to Rarefied Gas Dynamics 24th Symposium (July 2004)
  - [25] H. C. W. Beijerinck, G. H. Kaashoek, J. P. M. Beijers and M. Verheijen, Physica **121C**, 425 (1983)
  - [26] J. M. Standard and P. R. Certain, J. Chem. Phys. **83**, 3002 (1985)
  - [27] F. E. Cummings, J. Chem. Phys. **63**, 4960 (1976)
  - [28] R. Delhuille, C. Champenois, M. Büchner, L. Jozefowski, C. Rizzo, G. Trénec and J. Vigué, Appl. Phys. **B 74**, 489 (2002)
  - [29] J. Blanc et al., J. Chem. Phys. **96**, 1793 (1992)

- [30] C. J. Sansonetti, B. Richou, R. Engleman Jr and L. J. Radziemski, Phys. Rev. A **52**, 2682 (1995)
- [31] W. I. McAlexander, E. R. I. Abraham and R. G. Hulet, Phys. Rev. A **54**, R5 (1996)
- [32] T. W. Hänsch and B. Couillaud, Opt. Comm. **35**, 441 (1980)
- [33] J. Schmiedmayer, M. S. Chapman, C. R. Ekstrom, T. D. Hammond, D. A. Kokorowski, A. Lenef, R.A. Rubinstein, E. T. Smith and D. E. Pritchard, in Atom interferometry edited by P. R. Berman (Academic Press 1997), p 1
- [34] C. R. Ekstrom, J. Schmiedmayer, M. S. Chapman, T. D. Hammond and D. E. Pritchard, Phys. Rev. A **51**, 3883 (1995)
- [35] O. F. Hagen, Phys. Fluids **17**, 894 (1974)
- [36] W.C. Stwalley and L. H. Nosanow, Phys. Rev. Lett. **36**, 910 (1976)
- [37] J. De Boer and R.J. Lunbeck, Physica **XIV**, 520 (1948)
- [38] P. S. Julienne and F. H. Mies, J. Opt. Soc. Am. **B 6**, 2257 (1989)
- [39] R. Brühl and D. Zimmermann, Chem. Phys. Lett. **233**, 455 (1995)
- [40] R. A. Aziz, J. Chem. Phys. **99**, 4518 (1993)
- [41] K. T. Tang and J. P. Toennies, J. Chem. Phys. **118**, 4976 (2003)

FIG. 1: The reduced temperatures  $\tau_{X_i}$  are plotted as a function of the reduced z-coordinate  $\zeta$ . For  $\tau_{\parallel 1}$  and  $\tau_{\perp 1}$ , this plot is identical to figure 5 of Beijerinck and Verster [5]. The ultra cooling appears on  $\tau_{\parallel 2}$ , which reaches a terminal value lower than  $\tau_{\parallel 1}$ . The parallel and perpendicular temperatures of the seeded gas separate for larger  $\zeta$  values than the temperatures of the carrier gas and this fact is the basis of the ultra cooling of the seeded gas. The present calculation corresponds to the case of lithium seeded in argon, with  $\rho_s = 2.55$  and  $\rho_o = 1.32$ , and it predicts  $T_{\parallel 2\infty}/T_{\parallel 1\infty} = 0.38$ .

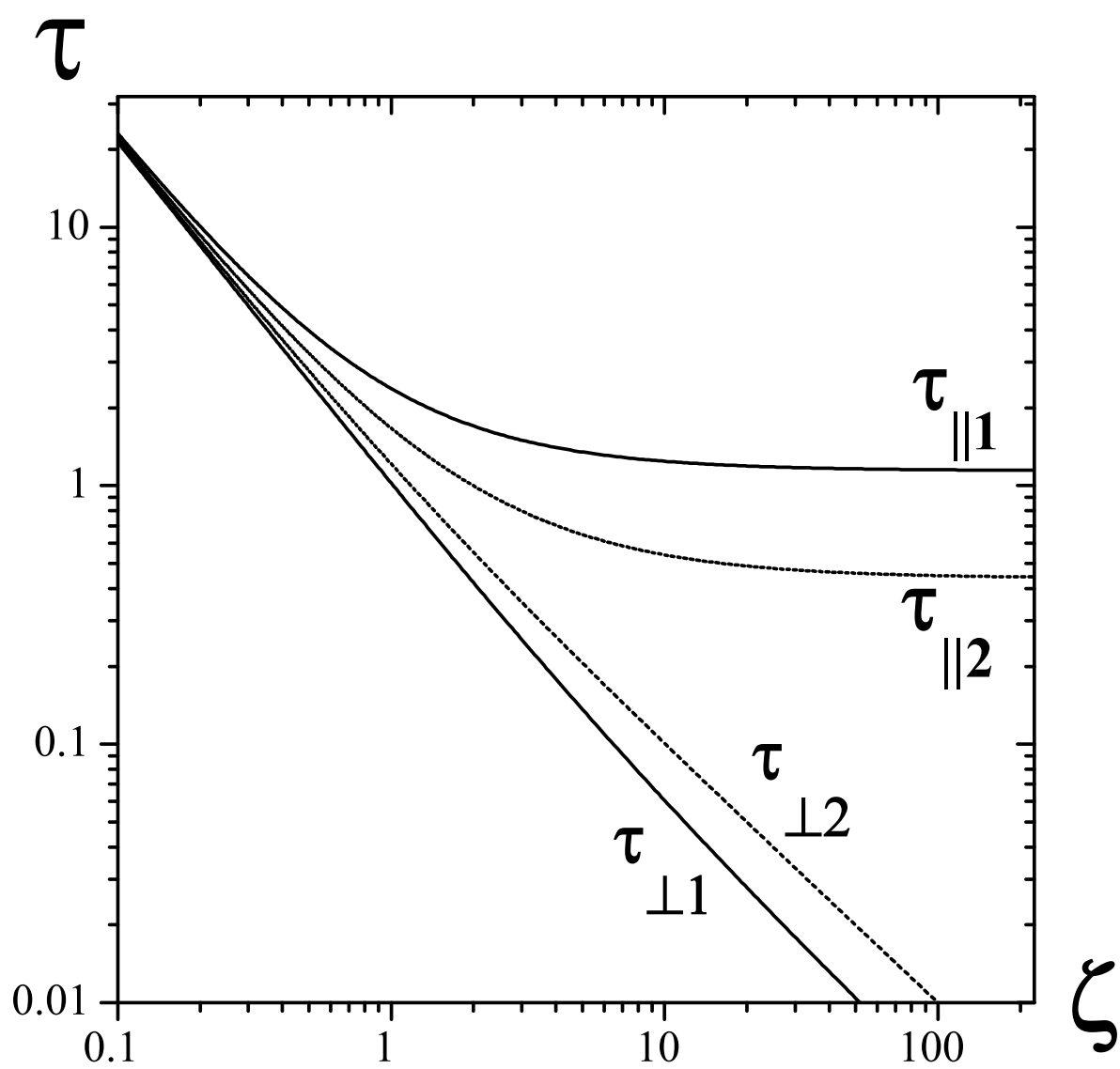
FIG. 2: The calculated parallel temperature ratio  $T_{\parallel 2\infty}/T_{\parallel 1\infty}$  is plotted as a function of the mass ratio  $m_2/m_1$ , spanning the range from hydrogen to rubidium seeded in argon. Each curve corresponds to a different value of the ratio  $\rho_s$  and is labeled by this value.

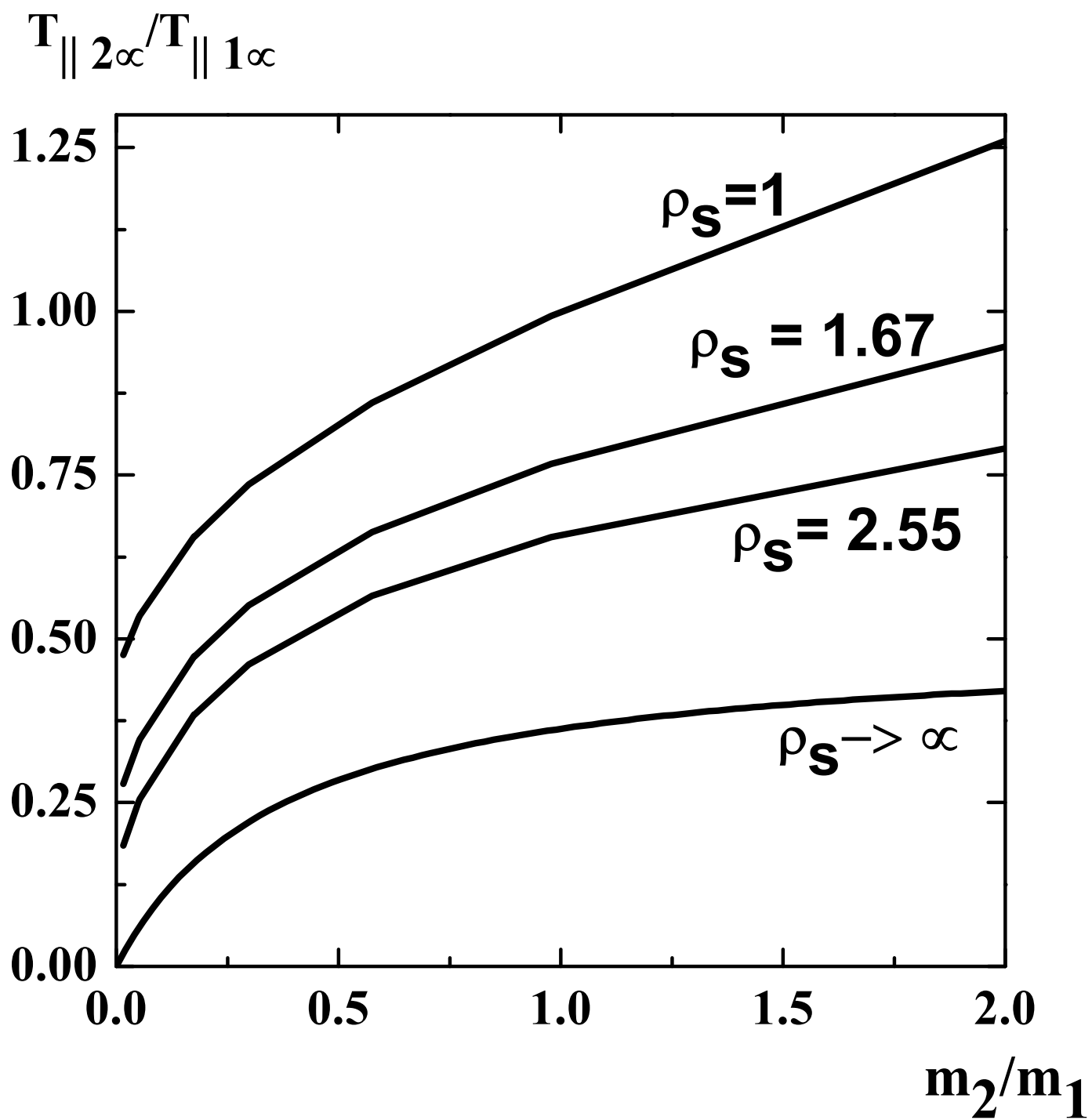
FIG. 4: The parallel temperature of lithium seeded in argon as a function of argon pressure in the source. The points represent our measurements. The full curve is the result of our theoretical calculation with  $T_{\parallel 2}/T_{\parallel 1} = 0.38$ . The agreement between theory and experiment is quite good. The dashed curve results from a fit of the four data points with an argon pressure below 400 millibar: the best fit corresponds to a temperature ratio  $T_{\parallel 2}/T_{\parallel 1} = 0.31$ . For larger source pressures, the lithium parallel temperature remains roughly constant, in disagreement with theory (see the discussion in the text).

FIG. 5: Plot of the variations of  $Y^{(l)} = Q^{(l)}(g)E^{*1/3}/\sigma^2$  as a function of  $E^*$  for  $l = 1$  (upper curve) and  $l = 2$  (lower curve). Both quantities approach their limit rapidly when  $E^* < 0.5$ .

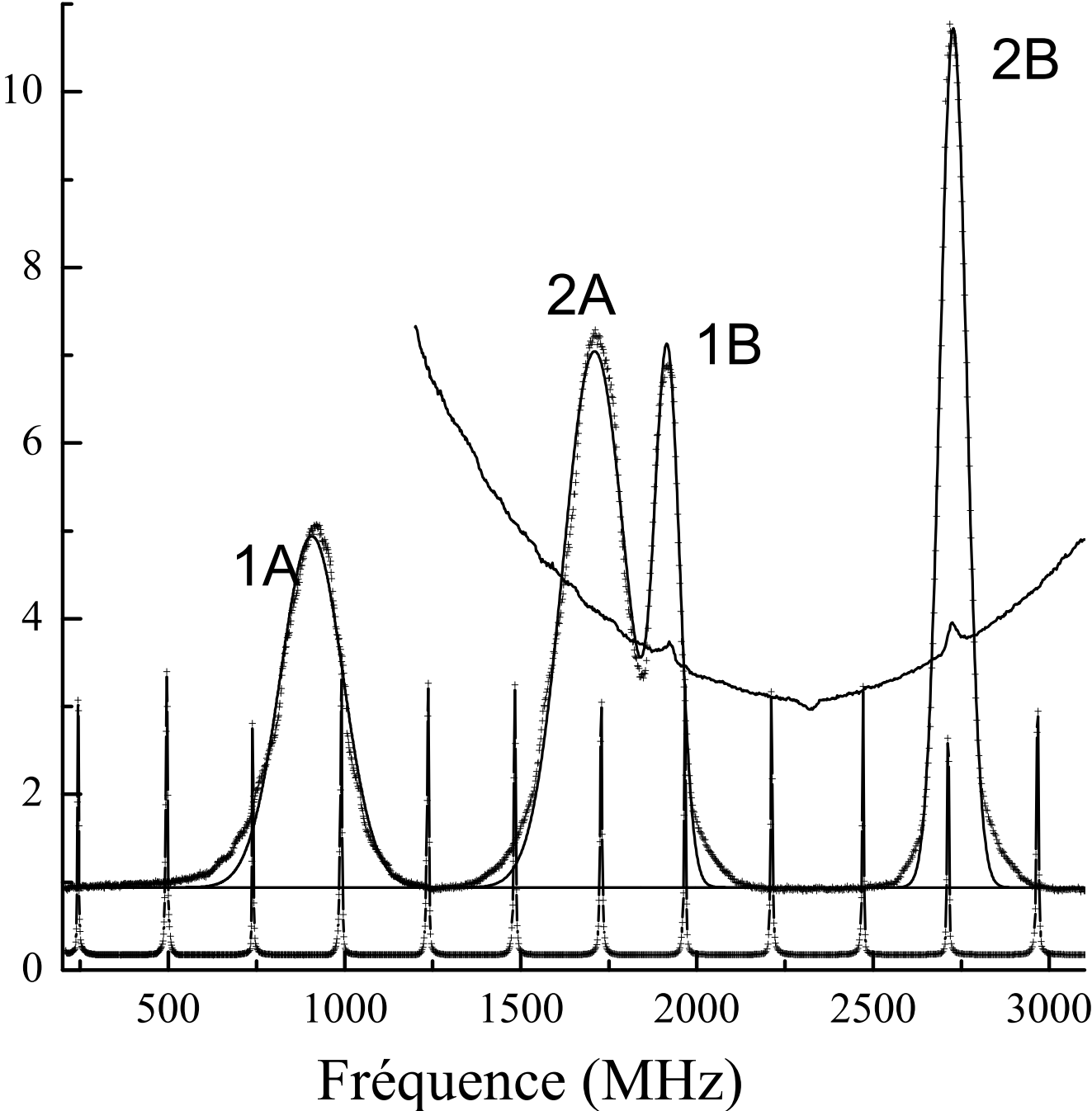
FIG. 6: Plot of the variations of the quantities  $C^{(l,s)}(T^*)$  defined by equation (40) as a function of  $T^* = k_B T/\epsilon$  for  $(l, s) = (1, 1)$  (dots);  $(1, 2)$  (dash-dotted curve) and  $(2, 2)$  (solid curve).

FIG. 3: Laser induced fluorescence signal as a function of the laser frequency: the dots represent the experimental data and the full curves are the Gaussian fits to each line. The Fabry-Perot used for calibration has a free spectral range equal to  $251.4 \pm 0.5$  MHz. The saturated absorption spectrum providing lithium Doppler-free peaks is represented for frequencies above 1250 MHz. The fluorescence peaks are labeled by the ground state  $F$  value ( $F = 1$  or  $2$ ) and by a letter corresponding to the laser beam. The angle between the atomic beam and the laser beam is  $\theta_A = 47.9 \pm 0.5^\circ$  for beam A and  $\theta_B \approx 90^\circ$  for beam B.

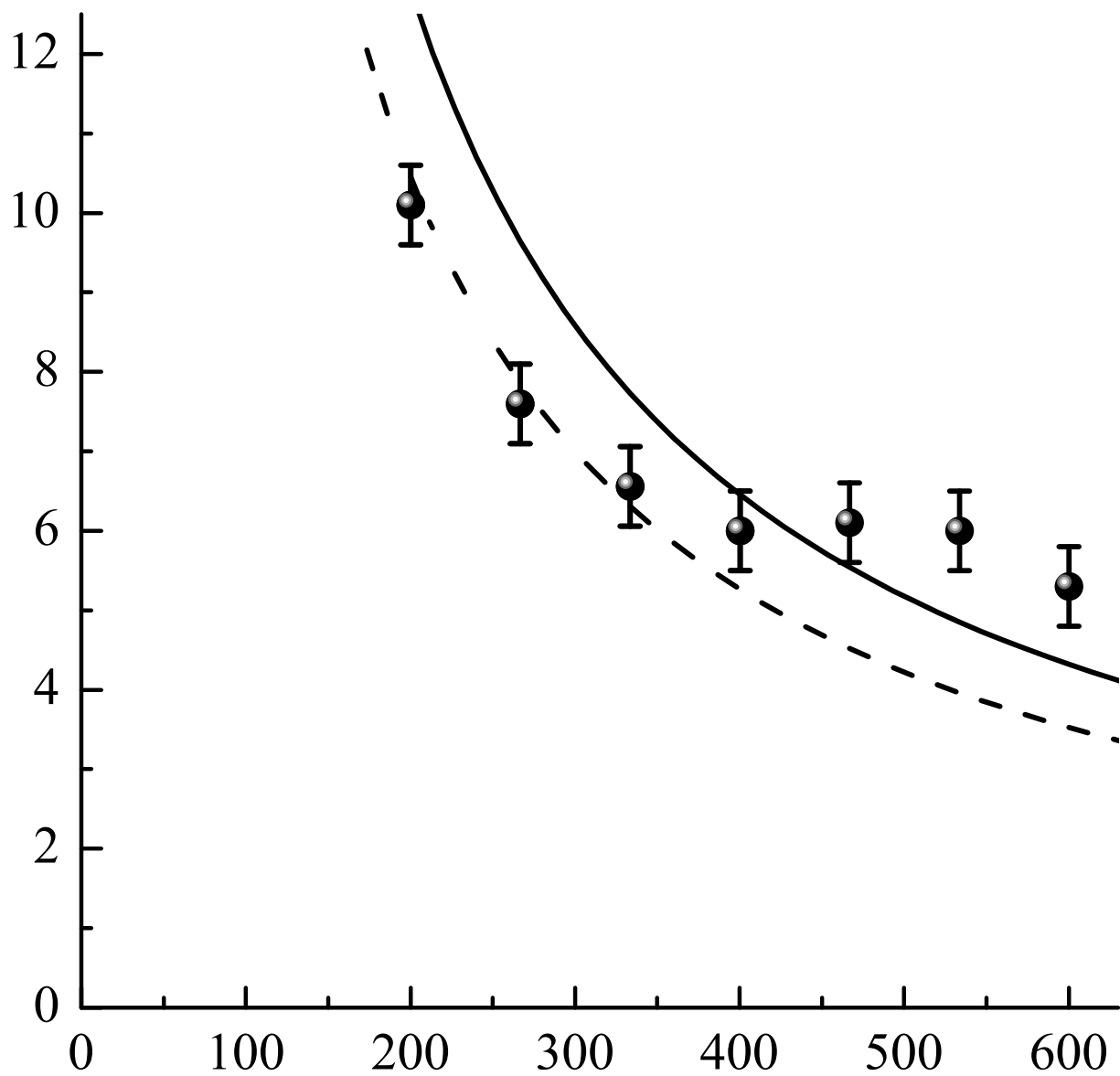




Signal (u.a.)



$T_{//2}$  (K)



Source pressure (mbar)

